Vaccine 37 (2019) 4204–4213

Contents lists available at ScienceDirect

Vaccine

journal homepage: www.elsevier.com/locate/vaccine

# Co-administration of GM-CSF expressing RNA is a powerful tool to enhance potency of SAM-based vaccines

Cristina Manara, Michela Brazzoli, Diego Piccioli, Marianna Taccone, Ugo D'Oro, Domenico Maione, Elisabetta Frigimelica *

*GSK Vaccines S.r.l., Via Fiorentina 1, 53100 Siena, Italy*

ARTICLE INFO

*Article history:*
Received 15 October 2018
Received in revised form 8 April 2019
Accepted 11 April 2019
Available online 18 June 2019

*Keywords:*
Self-amplifying mRNA
Protective immunity
Vaccine
Influenza
GM-CSF

ABSTRACT

Self-amplifying mRNAs (SAM)-based vaccines have been shown to induce a robust immune response in various animal species against both viral and bacterial pathogens. Due to their synthetic nature and to the versatility of the manufacturing process, SAM technology may represent an attractive solution for rapidly producing novel vaccines, which is particularly critical in case of pandemic infections or diseases mediated by newly emerging pathogens. Recent published data support the hypothesis that Antigen Presenting Cells (APCs) are responsible for CD8+ T-cell priming after SAM vaccination, suggesting cross-priming as the key mechanism for antigen presentation by SAM vaccines. In our study we investigated the possibility to enhance the immune response induced in mice by a single immunization with SAM by increasing the recruitment of APCs at the site of injection. To enhance SAM immunogenicity, we selected murine granulocyte-macrophage colony-stimulating factor (GM-CSF) as a model chemoattractant for APCs, and developed a SAM-GM-CSF vector. We evaluated whether the use of SAM-GM-CSF in combination with a SAM construct encoding the Influenza A virus nucleoprotein (NP) would lead to an increase of APC recruitment and NP-specific immune response. We indeed observed that the administration of SAM-GM-CSF enhances the recruitment of APCs at the injection site. Consistently with our hypothesis, co-administration of SAM-GM-CSF with SAM-NP significantly improved the magnitude of NP-specific CD8+ T-cell response both in terms of frequency of cytotoxic antigen-specific CD8+ T-cells and their functional activity *in vivo*. Furthermore, co-immunization with SAM-GM-CSF and SAM-NP provided an increase in protection against a lethal challenge with influenza virus. In conclusion, we demonstrated that increased recruitment of APCs at the site of injection is associated with an enhanced effectiveness of SAM vaccination and might be a powerful tool to potentiate the efficacy of RNA vaccination.



## 1. Introduction

In the last two decades, RNA-based vaccines have emerged as a promising alternative to the use of plasmid DNA (pDNA) and viral vectors for vaccine development [1–3]. They combine the flexibility of pDNA vaccines with the advantage of avoiding some limitations, such as potential integration into the host cell genome and anti-vector immunity [4–12]. Messenger RNA (mRNA) vaccines have demonstrated their potential also in active immunotherapeutic immunization protocols in cancer patients [3]. In the field of mRNA vaccines, the self-amplifying mRNA (SAM) platform has shown to be a powerful tool to develop vaccines against a wide range of both viral and bacterial pathogens [13].

SAM is derived from a modified alphavirus genome containing the genes encoding the non-structural proteins which allow RNA replication, whereas the structural protein sequences are replaced with a gene encoding an antigen of interest, which is abundantly expressed from a subgenomic promoter in the cytoplasm of cells transfected with SAM [5].

SAM vaccines have shown to be able to trigger potent humoral and cellular responses. In addition, thanks to the versatility of the manufacturing processes, SAM technology may represent an effective platform to rapidly produce vaccines against pandemic infectious diseases or newly emerging pathogens [6,14–17]. In this context, further optimization to improve the response after a single immunization would be beneficial.

Progress made in understanding the mechanism of action of SAM-based vaccines has demonstrated that following intramuscular injection, antigen expression mostly occurs in transfected

* Corresponding author.
*E-mail address:* elisabetta.x.frigimelica@gsk.com (E. Frigimelica).

https://doi.org/10.1016/j.vaccine.2019.04.028
0264-410X/

myocytes at the inoculation site. However, recent evidences suggest that the CD8+ T-cell priming is initiated by professional APCs rather than myocytes [18]. APCs are barely found in the normal muscle tissue but they are able to migrate to the site of inoculation in response to inflammatory or chemotactic signals [19]. Thus, infiltrating APCs might present the SAM expressed antigen to T-cells directly or through cross-presentation, in order to initiate the immune response.

Increasing the number of APCs at the injection site has proven to be a successful approach to enhance antigen uptake and presentation to T-cells [19–23]. In the recent years, Granulocyte-Macrophage Colony-Stimulating Factor (GM-CSF) has received considerable attention for its ability to induce recruitment, maturation and activation of APCs [24–29]. GM-CSF has proved to be efficacious as vaccine adjuvant in a number of immunization systems: administered as recombinant protein [30–34], encoded by plasmid DNA and viral vaccines [35–41], and expressed by transfected dendritic cells passively transferred both in the mouse model and in humans [42–44].

In the current study, we evaluated whether an enhancement in the number of APCs at the site of SAM administration could improve the efficacy of SAM vaccines. To this aim we co-administered a SAM encoding for mouse GM-CSF (SAM-GM-CSF) with a SAM encoding for Influenza A virus Nucleoprotein (SAM-NP). We selected NP as model antigen since both T-cell and antibody responses specific to NP delivered with SAM have been shown to be protective in a mouse model of influenza infection [15].

## 2. Results

### 2.1. Generation and characterization of SAM constructs

In order to demonstrate the importance of APC recruitment for the improvement of SAM vaccine efficacy, we selected murine GM-CSF as a model chemoattractant molecule and we used the Influenza A NP as the vaccine antigen. As negative control, a biologically inactive form of GM-CSF (mutGM-CSF) was obtained by point mutation at amino acidic positions 15 and 21, which are required for binding to the GM-CSF receptor [40,45]. All sequences were cloned into the SAM DNA plasmid backbone containing the promoter for the T7 bacteriophage RNA polymerase (Fig. 1a). Linear plasmid DNAs were transcribed into RNA through the *in vitro* transcription reaction and a guanine nucleoside (cap) was added to the 5′ terminus of primary RNAs. All replicons were tested for their capability to replicate *in vitro* with an in house developed *in vitro* potency assay (IVP): all constructs were able to induce around 25% of dsRNA positive cells, comparable to a reference RNA (20%, Fig. 1S). Antigen expression was evaluated on baby hamster kidney (BHK) cells electroporated with the three replicons. NP was detected in the cytosol of transfected cells with an anti-NP antibody (Fig. 1b).

To evaluate the expression of secreted GM-CSF and mutGM-CSF, Western Blot analysis with an anti-GM-CSF antibody was performed on supernatants collected 18 h after electroporation of BHK cells. Both proteins were revealed as multiple bands, one of the expected molecular weight of 14 kDa, as the positive control (commercial recombinant protein produced in *E. coli*), and two bands of higher molecular weight (Fig. 1c). Since GM-CSF is a highly glycosylated protein (two N-glycosylation sites and two O-glycosylation sites are reported), we verified whether the higher molecular weight bands were due to N-glycosylation of the protein. To this aim, the supernatant of electroporated BHK cells was treated with Peptide-N-glycosidase F (PNGaseF) and then analyzed by western blot. After deglycosylation, the high molecular weight bands disappeared, confirming that the protein bands identified as wild type or mutated GM-CSF are glycosylated forms of this cytokine (Fig. 2S). The biological activity of codon optimized GM-CSF and mutGM-CSF was confirmed *in vitro* by evaluating their ability to generate differentiated dendritic cells (DCs) from bone marrow derived monocytes (BMDM). A codon optimized, histidine-tag version of both wild type and mutated GM-CSF was purified from the supernatant of BHK transfected cells and compared to recombinant GM-CSF for the ability to induce DC differentiation. Both recombinant and codon optimized GM-CSF promoted the development of a comparable percentage of differentiated DCs (approximately 70%, Fig. 3S), while, as expected, cells cultured with the histidine-tag form of mutGM-CSF did not survive in culture.

### 2.2. Administration of SAM-GM-CSF promotes an enhanced transient recruitment of antigen presenting cells at the injection site

To evaluate the potential of SAM-GM-CSF to induce recruitment of APCs *in vivo*, SAM vectors were formulated with a cationic nanoemulsion (CNE) and used to immunize mice. Mice were injected intramuscularly with SAM-NP, SAM-NP + SAM-mutGM-CSF or with SAM-NP + SAM-GM-CSF. At different time points after the immunization (Fig. 4S-f), quadriceps muscles and inguinal draining lymph nodes were collected and immune cell infiltration was assessed by flow cytometry.

Mice injected with SAM expressing GM-CSF, compared to SAM-mutGM-CSF, showed a higher muscle cellular infiltrate between day 3 and 4 after the treatment, reaching the peak at day 4 (Fig. 2a). After that, the cell recruitment declined, returning to baseline level at day 25. Consequently, from day 7 the added value of GM-CSF in promoting cell recruitment was no longer observable. Before day 3 no major differences between the active and non-active form of GM-CSF were observed in the induction of cell recruitment (Fig. 2a). A detailed analysis of the different subpopulations of immune cells recruited at the injection site revealed that the majority of these cells consisted of APCs, either in presence or in absence of the active form of GM-CSF. Particularly, muscles of mice immunized with SAM-GM-CSF, compared to SAM-mutGM-CSF, showed an increased infiltration of macrophages and dendritic cells, with a peak at day 4 (Fig. 2, b and c), while no major differences were observed in the recruitment of monocytes (Fig. 2d).

Cell recruitment was analyzed also at the level of the inguinal draining lymph nodes. Differently from what observed at the site of administration, no significant variation was detected between the three immunization groups in the total number of immune cells recruited in the draining lymph nodes (Fig. 3).

Similar patterns of recruitment at the level of both muscles and draining lymph nodes were observed with a SAM vector encoding a different model antigen, such as OVA (SAM-OVA) (Fig. 4S and 5S), proving that SAM-GM-CSF ability to induce *in vivo* recruitment of APCs is independent on the antigen expressed by the co-administered vector.

In conclusion, RNA vaccination with a SAM construct containing GM-CSF increases recruitment of APCs, in particular DCs and macrophages, at the injection site, through a kinetic revealing the enhanced cell recruitment between 3 and 7 days after the immunization.

### 2.3. Effect of SAM-GM-CSF on the immune response to SAM-NP

With the aim to verify whether the increased number of APCs at the injection site may lead to an enhanced immunogenicity of the antigen, we characterized the immune response to NP in the different groups of mice. Firstly, we analyzed the T-cell response to our model antigen NP. Splenocytes were collected from immunized mice ten days after the injection and then stimulated *in vitro* with the H2-$D^b$ restricted $NP_{366-377}$ peptide or the recombinant NP

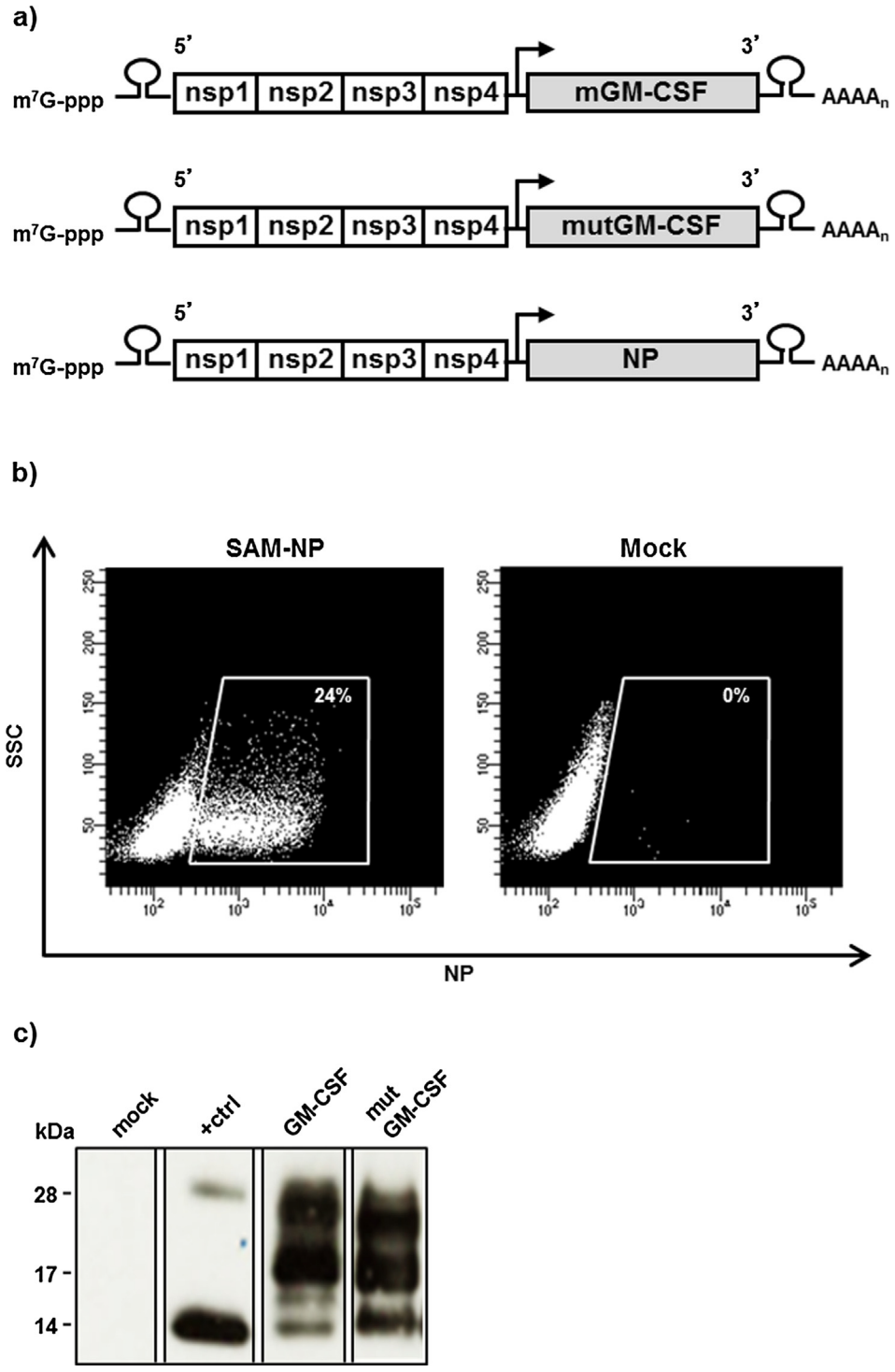


**Fig. 1.** Schematic representation of SAM vectors and *in vitro* characterization. (a) SAM-GM-CSF, SAM-mutGM-CSF and SAM-NP constructs contain a 5′ cap, four non-structural genes (nsp1-4), a 26S subgenomic promoter (black arrow), the antigen of interest and a 3′ polyadenylated tail. (b) Frequency of NP-expressing BHK cells transfected with mock or SAM-NP replicon were analyzed by flow cytometry. (c) Western Blot showing expression of GM-CSF and mutGM-CSF in supernatants from transfected BHK cells. Recombinant GM-CSF protein purified from *E. coli* (Miltenyi Biotec) was added as positive control. Mock, non-transfected cells, were added as negative control.

protein. The frequencies of NP-specific CD4+ and CD8+ T-cells were determined by measuring the frequencies of IFN-γ, TNF-α and IL-2 producing T-cells, by flow cytometry analysis.

As shown in Fig. 4a, co-administration of SAM-GM-CSF with SAM-NP in immunized mice was able to elicit higher frequencies of NP-specific CD8+ T cells, whereas in the presence of SAM-mutGM-CSF no increase of NP-specific CD8+ T-cell response was observed compared to SAM-NP alone. However, the increase of CD8+ T-cell response was not associated to a change in the cytokine profile, since in all immunized groups of animals the NP-specific CD8+ T-cells were mainly IFN-γ+ and IFN-γ+/TNF-α+, a phenotype generally associated to an effector function. To confirm the cytotoxic phenotype of the induced CD8+ T-cells, we measured the frequency of CD8+ T-cells expressing CD107a, a degranulation marker.

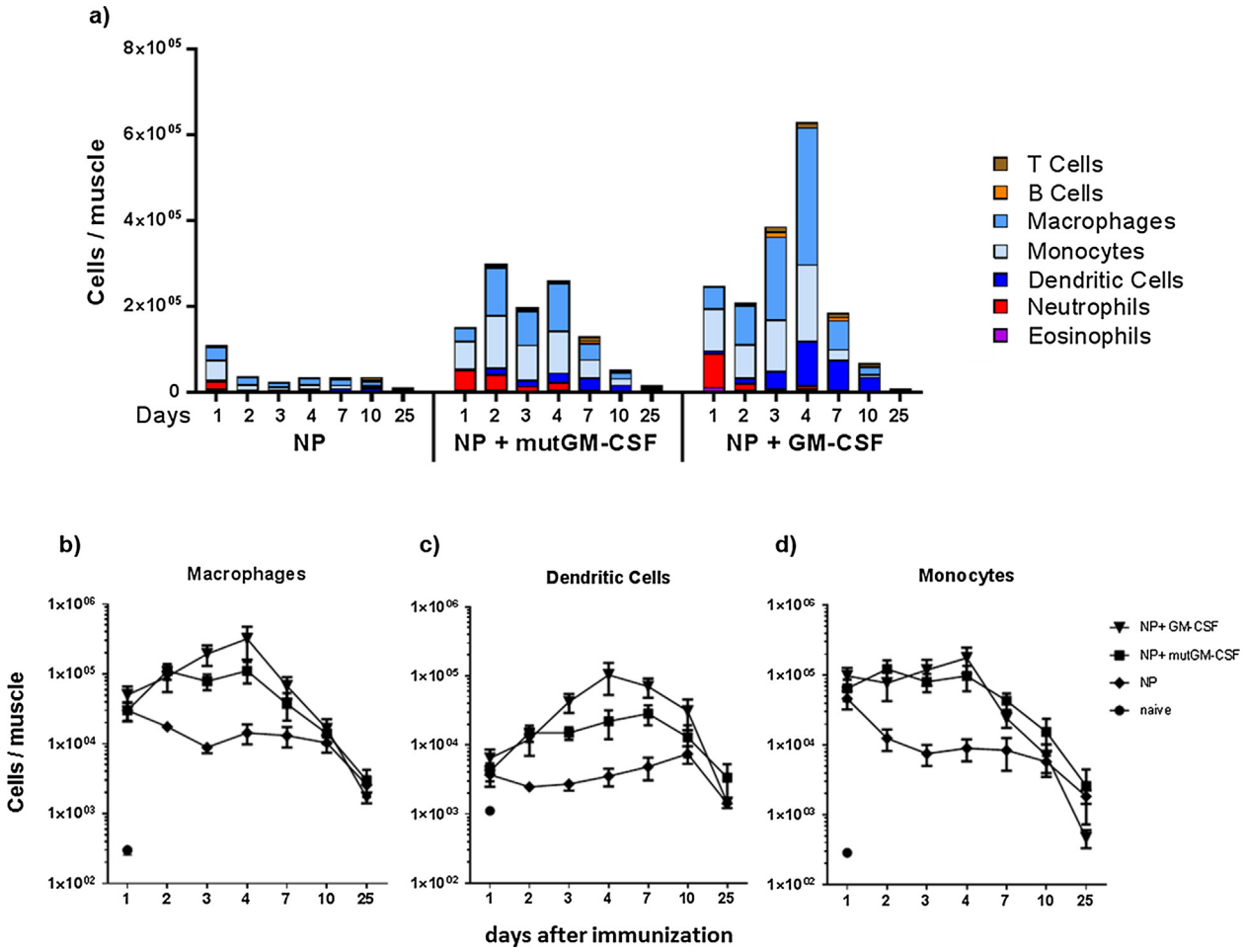


**Fig. 2.** Cell recruitment following SAM immunization at the injection site. Groups of four mice per treatment were injected i.m. with 1.5 μg SAM-NP, 1.5 μg SAM-NP + 1.5 μg SAM-mutGM-CSF or 1.5 μg SAM-NP + 1.5 μg SAM-GM-CSF. Mice were sacrificed at the indicated time points and single cell suspensions from the entire treated muscles were obtained by enzymatic digestion. Immune cell composition of the entire muscle was assessed by flow cytometry, as reported in Materials and Methods. (a) Bars show cumulative number of immune cell types at different days after the immunization with SAM-NP, SAM-NP + SAM-mutGM-CSF or SAM-NP + SAM-GM-CSF, as indicated. Individual color code indicates mean number of respective cell type, as reported in the legend, counted in the whole treated muscle. (b)–(d) The curves represent the mean of the total cell counts in the whole treated muscle ± SEM, of macrophages (b), dendritic cells (c) and monocytes (d) along the time course.

Indeed, approximately 90% of the total NP-specific CD8+ T-cells induced by the immunization resulted positive for CD107a (Fig. 4b).

When the CD4 + T-cell response was analyzed, mice receiving SAM-GM-CSF + SAM-NP showed only a modest and not relevant increase in total NP-specific CD4 + T-cells (Fig. 4c). Similarly to CD8+ T-cell response, the phenotype of cytokine secreting CD4+ T cells is roughly the same throughout the immunized groups (Pie charts, Fig. 4a and 4c).

The humoral response was characterized in the mouse sera collected three weeks after the immunization and analyzed for the presence of NP-specific IgG (Fig. 4d). Consistently with the observation that the addition of SAM-GM-CSF has no major effect on the CD4+ T-cell response, all the different SAM-NP combinations elicited comparable levels of anti-NP IgG titers, demonstrating that the expression of GM-CSF by SAM does not potentiate the induction of the antigen-specific antibody response.

Taken together, all these evidences demonstrate that RNA immunization using SAM-GM-CSF improved the effector CD8+ T-cell response, while not affecting the humoral immune response.

### 2.4. SAM-GM-CSF strenghtens SAM vaccination efficacy in vivo

To assess the cytotoxic potential of the increased NP-specific CD8+ T-cells generated by SAM-GM-CSF co-administration, we performed an *in vivo* cytotoxicity assay. Splenocytes from naïve mice were labeled with CFSE, pulsed with the H2-D$^b$ restricted NP peptide $NP_{366-377}$ and intravenously injected in mice previously immunized with the different combinations of SAM-NP. As control, an equal number of splenocytes labeled with CMTMR and pulsed with $OVA_{257-264}$ peptide were concomitantly injected. The following day, the frequencies of CFSE+ and CMTMR+ cells recovered from spleens were determined in order to quantify the specific CD8+ T-cell lytic activity. Co-administration of SAM-GM-CSF + SAM-NP resulted in a stronger cytolytic activity with almost 100% specific lysis, while both SAM-NP and SAM-NP + SAM-mutGM-CSF immunized mice showed a lower level of cytotoxicity, with a specific lysis of about 82%. No specific lysis was detected in PBS treated mice confirming the antigen-specificity of the cytotoxic activity (Fig. 5a). CD8+ cytotoxic T-cells have been reported to play an important role in protection from lethal influenza virus challenge in mice [46,47]. Thus, it would be appropriate to use this animal model to evaluate the capacity of SAM-GM-CSF co-administration to improve the protection efficacy of the SAM-NP vaccine against influenza. We assessed, therefore, the effect of SAM-GM-CSF on protection efficacy induced with SAM-NP vaccination by challenging mice with a lethal dose of PR8 influenza A virus after immunization with the different SAM-NP combinations. Survival, body weight loss and clinical signs of illness were

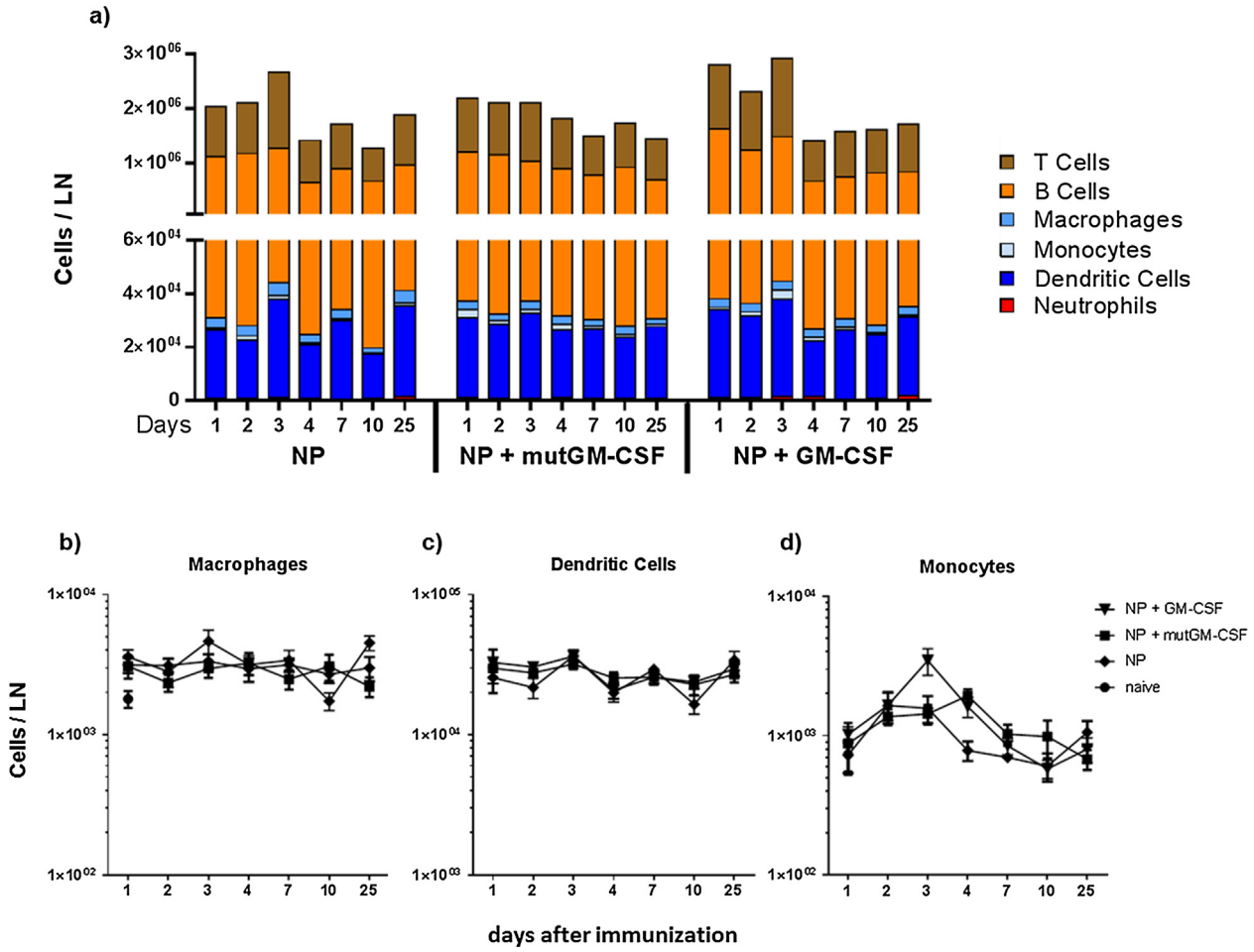


**Fig. 3.** Cell recruitment following SAM immunization in the draining lymph nodes. Groups of four mice per treatment were injected i.m. with 1.5 μg SAM-NP, 1.5 μg SAM-NP + 1.5 μg SAM-mutGM-CSF or 1.5 μg SAM-NP + 1.5 μg SAM-GM-CSF. Mice were sacrificed at the indicated time points and single cell suspensions from the entire lymph nodes were obtained by enzymatic dissociation. Immune cell composition of the entire lymph nodes was assessed by flow cytometry, as reported in Materials and Methods. (a) Bars show the cumulative number of immune cell types at different days after the immunization with SAM-NP, SAM-NP + SAM-mutGM-CSF or SAM-NP + SAM-GM-CSF, as indicated. Individual color code indicates the mean number of respective cell type, as reported in the legend, counted in the whole lymph nodes. (b)–(d) The curves represent the mean total cell counts per lymph node ± SEM of macrophages (b), dendritic cells (c) and monocytes (d) along the time course.

monitored for fourteen days after the infection of previously immunized mice. All mice immunized with SAM replicons expressing NP, either alone or in combination with active or mutated form of GM-CSF, showed a significantly higher survival rate compared to PBS-treated control mice. However, SAM-GM-CSF co-administration was able to increase the SAM-NP conferred protection, even if the observed difference was not statistically significant. In particular, a 78% survival rate was observed in mice receiving SAM-GM-CSF + SAM-NP versus 62% survival observed in mice immunized with SAM-NP alone and 55% in mice that received the mutant GM-CSF (Fig. 5b).

In conclusion, our study shows that immunization with a SAM vaccine containing a construct encoding for GM-CSF leads to an increased recruitment of APCs at the injection site, which correlates with the potentiation of an effective antigen-specific CD8+ T-cell response.

## 3. Discussion

Conventional vaccines are not particularly efficient at eliciting a strong CD8+ T-cell response, which is fundamental for clearing certain type of infections. An effective CD8+ T-cell response against conserved antigenic epitope, for example, is of particular importance when humoral immunity induced by previous infections or vaccination is inadequate for protection against a newly emerging pathogenic strain. Cytotoxic T-lymphocytes have the capability to recognize and kill virus-infected cells, facilitating virus clearance. In this light, vaccines promoting cell-mediated immunity should be considered as a potent weapon to fight newly emerging and potentially highly pathogenic viruses [48].

SAM vaccines have, indeed, emerged as an attracting technology platform able to generate potent, versatile and easily produced vaccines to address the health challenges of the 21st century [49]. Thanks to their fully synthetic nature and to the versatility of the manufacturing process, SAM vaccines can be produced in large amounts within few days from the identification of an antigen sequence. Their capacity to express high levels of the antigen of interest into the cytoplasm of host cells allows them to trigger both, antibody-mediated and cell-mediated immunity. SAM vaccines are especially efficient in the induction of a strong and effective CD8+ T-cell response [13,15,16]. It has been postulated that for CD8+ triggering SAM mechanism of action works via cross-priming, following the apoptosis of transfected myocytes and the consequent release of the antigen-associated apoptotic bodies that should be phagocytosed by APCs and presented via the MHC class I. Nevertheless, direct transfection of APCs *in vivo* cannot be excluded [18]. Whatever it is the mechanism driving the response to this vaccine, the presence of APCs at the site of injection seems critical

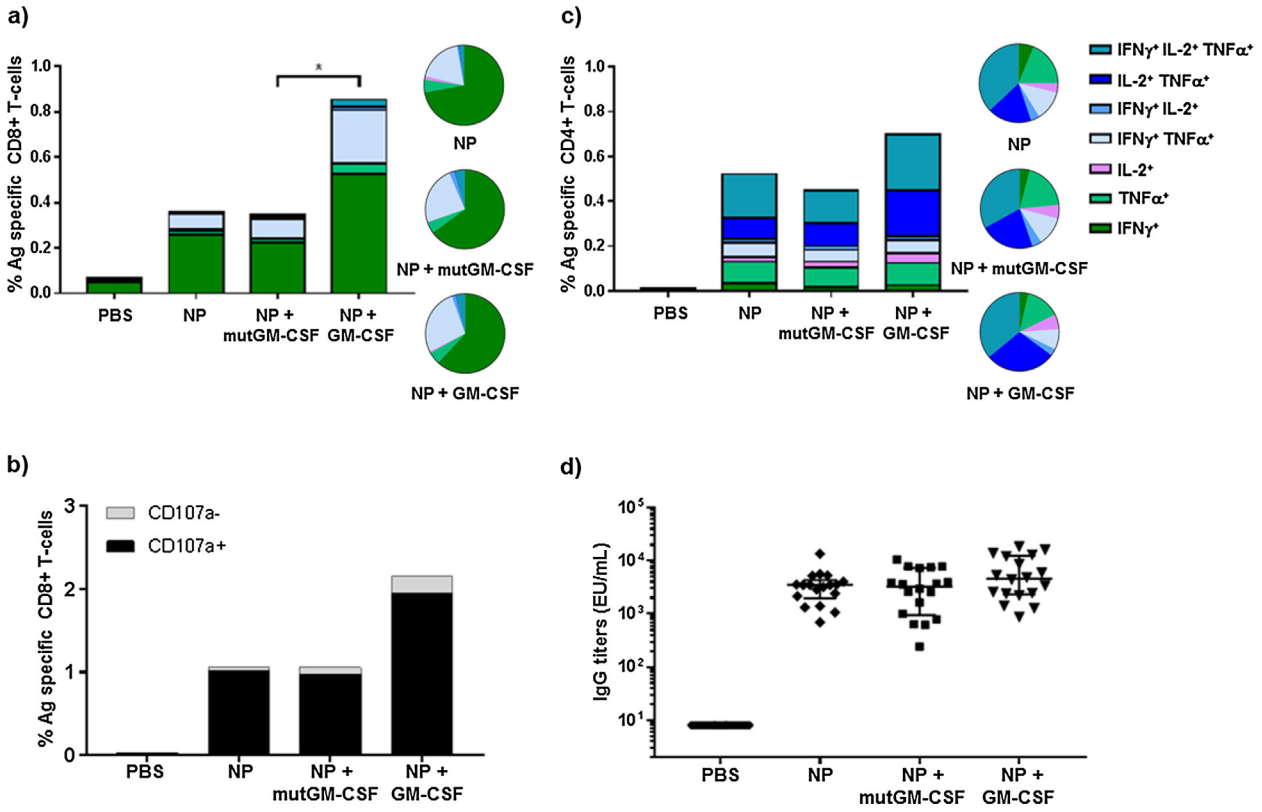


**Fig. 4. Immunogenicity of SAM Vaccines.** C57BL/6 mice (six/group) were immunized i.m. with 1.5 μg of SAM-NP, 1.5 μg SAM-NP + 1.5 μg SAM-mutGM-CSF or 1.5 μg SAM-NP + 1.5 μg SAM-GM-CSF. Ten days after the immunization, the frequency of Ag-specific, cytokine-secreting CD8+ (a) or CD4+ (c) T-cells was determined by flow cytometry on splenocytes stimulated *in vitro* with the $NP_{366-377}$ peptide. Bars represent the mean frequency, color code indicates the different combinations of cytokines produced by the respective cells. Statistical analysis was performed using the Mann-Whitney *U* test, *p < 0.05. Pie charts depict the relative percentage of Ag-specific T-cells producing each cytokine combination. (b) Surface expression of CD107a was assessed by flow cytometry on splenocytes stimulated *in vitro* with $NP_{366-377}$. Bars show the frequency of cytokine-secreting CD8+ T-cells that express (black bars) or not (grey bars) CD107a. (d) Sera from single mice (eighteen mice/group) were collected three weeks after the immunization and analyzed for NP-specific total IgG titers. Individual mice, median with IQR are reported.

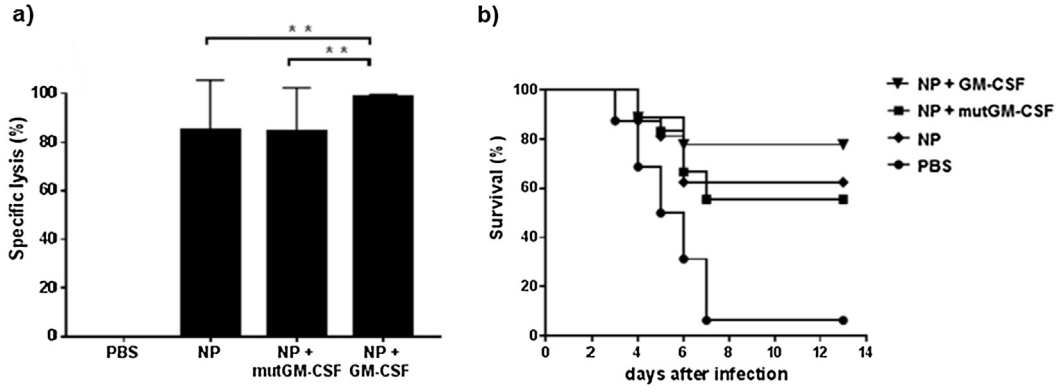


**Fig. 5.** Analysis of SAM-GM-CSF impact on *in vivo* functionality of SAM-NP vaccine. C57BL/6 mice were injected i.m. either with 1.5 μg SAM-NP, 1.5 μg SAM-NP + 1.5 μg SAM-mutGM-CSF or 1.5 μg SAM-NP + 1.5 μg SAM-GM-CSF. (a) *In vivo* cytotoxicity assay: the induction of NP-specific cytotoxic CD8+ T-cells by each treatment was characterized by FACS ten days after the immunization. Bars represent the percentage of *in vivo* NP-specific target cell lysis calculated for each immunization group (six mice/group). Data show mean of single mice ± SD. Statistical analysis was performed using Mann-Whitney *U* test. *, P < 0.05; **, P < 0.01. (b) Mouse model of protection against lethal influenza challenge: four weeks after the immunization, mice (sixteen/group) were challenged i.n. with the PR8 influenza virus. Graph represents survival percentage, monitored for fourteen days post-infection. Data show mean of single mice derived from two separate and merged experiments.

for SAM to induce a potent immune response to the encoded antigen.

In the present study we explored the possibility to improve the efficacy of SAM vaccination by increasing the number of APCs at the site of inoculation. We employed the SAM platform to express GM-CSF as model chemoattractant and NP from influenza A virus as our model antigen. GM-CSF has received considerable attention in the recent years for its ability to induce recruitment, maturation and activation of APCs and has proved to be efficacious as a vaccine adjuvant in a number of immunization systems. The synthetic SAM vectors were formulated using a non-viral delivery system based on CNE [50]. Our results show that, in the mouse system, co-administration of SAM encoding for a model antigen with SAM encoding for an active form of GM-CSF is able to induce, *in vivo*,

a transient higher recruitment of immune cells at the injection site, compared to co-administration with SAM encoding for a non-active mutated form of GM-CSF. The superiority of SAM-GM-CSF over the SAM-mutGM-CSF demonstrated that the effect observed is due to the biological activity of GM-CSF. In mice immunized with SAM encoding NP alone, recruitment of immune cells at the injection site was reduced and more transient compared to mice immunized with addition of SAM-mutGM-CSF, resolving very quickly within 48 h. Most likely this finding depends on the amount of CNE formulated RNA, which is known to promote innate immune response [50] and that in the SAM-NP alone group is half compared to the group immunized with the two SAM vectors. The cells recruited at the injection site were prevalently represented by APCs in both groups immunized with SAM-GM-CSF or SAM-mutGM-CSF associated to SAM-NP. However, the observed increase in the total number of infiltrated cells, when immunizing in the presence of SAM-GM-CSF, was predominantly mediated by recruitment of DCs and macrophages. These two cell types showed a similar kinetic of recruitment, reaching the peak of muscle infiltration between 3 and 7 days after the immunization. Interestingly, no effect of RNA administration was observed in the recruitment of immune cells within the draining LNs, suggesting that RNA immunization may exert its triggering of innate immune responses only at the injection site. The effect of GM-CSF on the recruitment of immune cells at the site of injection was independent of the antigen expressed by the co-administered SAM vector, as confirmed by results obtained using a co-administered vector encoding for a different model antigen, such as OVA.

When we investigated the impact of SAM-GM-CSF co-administration on NP immunogenicity, we did not observe an effect on the NP-specific IgG titers compared to animals co-administered with SAM-mutGM-CSF or treated with SAM-NP alone. Consistently neither a relevant increase in the frequencies of cytokine producing antigen-specific CD4+ T-cells, nor noteworthy differences in CD4+ T cell cytokine profile were observed in mice immunized with SAM encoding the model antigen co-administered with biologically active SAM-GM-CSF. However, a significant increase in the frequency of NP-specific cytokine producing CD8+ T-cells was observed in mice immunized with SAM-NP co-administered with SAM-GM-CSF, compared to mice immunized with SAM-NP alone or co-administered with SAM-mutGM-CSF, indicating that the administration of SAM encoding an active form of GM-CSF has an impact predominantly on the CD8+ component of the cellular arm of the immune response. The presence of SAM-GM-CSF affected the magnitude, more than the quality of the cellular response, because in all immunization groups CD8+ T-cells showed a similar cytotoxic and effector phenotype. Importantly, the higher frequency of NP-specific CD8+ T-cells following immunization in the presence of SAM-GM-CSF was associated to an augmented *in vivo* cytotoxic activity and an increased protection from a lethal dose of influenza A virus, in line with the fact that, in the mouse model, the NP-specific cytotoxic T lymphocytes are involved in influenza viral clearance [46,47].

Our study shows a partial correlation between a transient increase of cell recruitment at the injection site and the potentiation of an effective antigen-specific CD8+ T-cell response. Indeed, an increase in cellular infiltrate, although lower, was observed also in case of co-administration of SAM-mutGM-CSF with SAM-NP compared to administration of SAM-NP alone. As discussed above, we believe that in this case a greater cell recruitment may be due to the injection of a double dose of CNE formulated RNA. Nevertheless, the NP-specific CD8+ T-cell response was not amplified by co-administration of SAM-mutGM-CSF. Thus, the expansion of CD8+ T-cell response associated to co-administration of SAM-GM-CSF may be due to a specific biological activity of GM-CSF.

Our findings further underline the importance of CD8+ T-cells in the immune response induced by SAM vaccination. We observed an association between the increased recruitment of APCs at the site of injection, specifically promoted by GM-CSF, and the potentiation of an effective antigen-specific CD8+ T-cell response, without affecting the CD4+ T-cell response and the humoral immune response. The mechanism underlying these results deserves further investigation. A possible explanation, besides the increase of APC recruitment at the injection site per se, could be the induction by SAM-GM-CSF of mature dendritic cells and the promotion of antigen cross-presentation, as already hypothesized in the case of an anti-cancer immune response [51]. Whether dendritic cells activation occurs in the draining lymph nodes or at the site of injection still remains to be elucidated. In addition, investigating the phenotype of the recruited DC subtypes may help to elucidate the potential role of DCs in the induction of the potentiated effective CD8+ T-cell response.

In conclusion, our results demonstrate for the first time that the SAM platform can be exploited to express endogenous cytokines like GM-CSF as immunopotentiators. Future studies are needed to evaluate if SAM mediated expression of other cytokines is able to potentiate the immune response triggered by a SAM-based vaccine. Emerging infectious diseases, pandemics, and bioterrorism carry the potential for catastrophic impact. Thus, producing medical countermeasures against such threats is a big challenge for the scientific community [52]. Improving the potency of the SAM based vaccines might be a highly attractive strategy, especially to obtain a quick and effective response in case of outbreaks, when an increase in the magnitude of the response after a single administration is desirable. To this aim, we propose that the use of cytokines like GM-CSF in the design of SAM vaccines may be a useful tool to potentiate the effectiveness of RNA vaccination.

## 4. Materials and Methods

### 4.1. RNA synthesis of SAM GM-CSF and mutGM-CSF vectors

DNA plasmids encoding the self-amplifying RNAs were constructed as follows. Briefly, DNA encoding the mouse GM-CSF protein was codon optimized for expression in mouse (GeneArt). To obtain the inactive form of GM-CSF, the coding sequence of GM-CSF was mutated at amino acids 15 (H to A) and 21 (E to A) by PCR SOEing. The plasmid encoding the SAM-NP was described previously [15]. DNA was cloned into Sal I and Not I sites of an optimized replicon construct. RNA was prepared as previously reported [5].

### 4.2. BHK cells transfection and analysis of protein expression

Expression of GM-CSF, mutGM-CSF and NP proteins from SAM vectors was confirmed after transient transfection of BHK cells. $10^6$ BHK cells were electroporated (120 V, 25 ms pulse) with 200 ng of RNA and incubated at 37 °C and 5% $CO_2$. 18 h post transfection supernatants and cells were collected. To evaluate GM-CSF and mutGM-CSF expression, supernatants from transfected cells were resolved under reducing conditions on a 4–12% Bis-Tris polyacrylamide gel in MOPS electrophoresis buffer (Life Technologies) and blotted to nitrocellulose membrane (Life Technologies). GM-CSF and mutGM-CSF were visualized using a polyclonal rabbit anti mouse-GM-CSF antibody (Abcam). To evaluate NP expression, cells were trypsinized and stained with the Live/Dead Fixable Yellow viability marker (Molecular Probes-Life Technologies). Cells were then fixed and permeabilized with Cytofix/Cytoperm (BD Biosciences), washed with Perm-wash buffer (BD Biosciences) and stained with a FITC-labelled anti-NP antibody (Thermo Fisher

Scientific). Stained cells were acquired on a CANTO II flow cytometer (BD Biosciences) and analyzed with FACS Diva Software (BD v8.0.1).

### 4.3. Animal in vivo studies

Five weeks-old female C57BL/6 mice were immunized once intra muscularly (i.m.) in the quadriceps muscles of both hind legs (25 μl vaccine formulation per leg) with 1.5 μg of SAM-NP CNE56 or 3 μg of (SAM-NP CNE56 + SAM-mutGM-CSF CNE56) or (SAM-NP CNE56 + SAM-GM-CSF CNE56). Negative control mice were left untreated or injected intra muscularly with PBS. Muscle tissue and lymph nodes were collected at different time points as reported below. Sera were collected at day 21 post immunization, spleens were sampled at day 10 post immunization.

### 4.4. CNE/RNA formulation

CNE56 was prepared as previously described [50]. Each RNA was formulated independently as follows: RNA was diluted in the appropriate buffer at a concentration of 300 μg/ml and was then added to an equal volume of CNE. The complex was mixed gently and allowed to complex on ice for 30 min. Prior to administration, formulations were diluted to dosing concentrations and mixed when indicated. Formulations were characterized for particle size and RNA integrity (using gel electrophoresis) as previously described [50]. Dynamic light scattering was used to determine CNE particle size. CNE was diluted 1:500 in PBS and added to disposable low volume cuvettes (Malvern). Samples were measured on a Malvern NanoZs Zetasizer with a backward angle measurement using "PBS" as a dispersant (RI = 1.330). For RNA integrity, the RNA was extracted from the CNE56 by addition of 25 μl formulated sample to 475 μl isopropanol (Sigma). After 30 min of centrifugation at maximum speed, the pellet was suspended in nuclease free water (Ambion) and 1X Glyoxal Loading Dye (Ambion). The RNA was analyzed by gel electrophoresis on mini gel (MOPS/Sodium Acetate/EDTA buffer) 1% agarose and run at 100 V.

### 4.5. Ethical statements

All animal studies were conducted at the GSK Vaccines Animal Research Center, in compliance with the ARRIVE guidelines, the current Italian legislation on the care and use of animals in experimentation (Legislative Decree 116/92), and with the GSK Animal Welfare Policy and Standards. The animal protocols were approved by the Animal Welfare Body of GSK Vaccines, Siena, Italy, and by the Italian Ministry of Health (Approval number AEC 2014/05 and AEC 2015/01).

### 4.6. Immune cell infiltrate in quadriceps muscles and draining lymph nodes

C57BL/6 mice aged 5–6 weeks (four mice per group) were inoculated in the quadriceps muscles of the two hind legs (25 μl per site) on day 0. On day 1, 2, 3, 4, 7, 10 and 25, mice were sacrificed and both quadriceps muscles and draining inguinal lymph nodes were collected. Organs were then dissociated into single cell suspensions and analyzed by flow cytometry for immune cell infiltrate composition. To obtain single cell suspension, quadriceps muscles were digested with the enzyme mix provided by the Skeletal Muscle Dissociation kit (Miltenyi) for 1 h at 37 °C under constant agitation. The resulting cell suspensions were centrifuged, resuspended in Dulbecco's modified Eagle's medium (Gibco) and filtered through 70 μm nylon mesh (BD) before staining. Lymph nodes were dissociated by using a mix of Liberase DL Research Grade (Roche) and DNAse I (Sigma) for 90 min at 37°. The resulting cell suspensions were filtered through a 30 μm filter and then washed with PBS before staining. Total single cell suspensions were stained with Live Dead Yellow (Invitrogen) and the following fluorescently labeled antibodies: anti-Ly6C FITC, anti-CD11b PE-Cy7, anti-Ly6G PE, (all from BD Pharmingen), anti-MHCII AlexaFluor700, anti-F4/80 eFluor450, anti-CD11c APC-AlexaFluor780 (all from eBioscience) and anti-CD3 PerCPCy5.5 (BD Biosciences). The markers used allowed us to identify neutrophils (Ly6G high), eosinophils (Ly6G int, F4/80 int, SSC high), monocytes (CD11b high, CD11c−, Ly6C high), mDCs (CD11b high, CD11c+, MHCII+), macrophages (CD11b+, F4/80 high), and finally T cells (CD11b−, CD3+) and B cells (CD11b−, CD3-, MHCII+). All stained cells were acquired on a LSR II Special Order System flow cytometer (BD Biosciences) and analyzed using BD DIVA software (BD Bioscience). The different cell populations were identified as previously described [53].

### 4.7. Intracellular cytokine staining

Briefly, 1.5 x$10^6$ splenocytes were incubated for 6 h with the H2-$D^b$-restricted NP peptide ASNENMETMESS (2.5 μg/ml; JPT) and the recombinant NP protein (5 μg/ml; Sino Biological Inc.) in complete RPMI medium containing anti-CD107a FITC (BD Biosciences). Brefeldin A (Sigma) at 5 μg/ml was added for the last 4 h. The cells were then stained with Live/Dead Near (Invitrogen), fixed and permeabilized with Cytofix/Cytoperm (BD Biosciences), and further incubated with anti-CD16/CD32 Fc-Block (BD Biosciences). T-cells were stained with anti-CD3 APC, anti-CD4 V500, anti-IFN-γ BV785, anti–IL-2 PECy5, anti-TNFα BV605 (all from BD Biosciences), anti-CD44 V450 (BD Horizon) and anti-CD8 PE-Texas Red (Invitrogen). Cells were then acquired on a LSRII special order flow cytometer (BD Biosciences), and data were analyzed using FlowJo software version 9.9.5 (LLC).

### 4.8. Determination of NP-specific serum antibody by Enzyme-linked immunosorbent assay (ELISA)

NP-specific serum IgG titers were determined on individual sera collected three weeks after the immunization. Maxisorp plates (Nunc) were coated overnight at 4 °C with 2.3 μg/ml of NP (Sinobiological) and blocked with PBS, 1% BSA for 2 h at 37 °C. Serum samples and a standard serum, 2-fold serially diluted in PBS, 1% BSA, 0.05% Tween20, were transferred into coated and blocked plates and then incubated 2 h at RT. To detect antigen-specific IgG antibodies, plates were incubated with alkaline phosphatase-conjugated goat anti-mouse IgG (Sigma) for 2 h at RT. P-nitrophenyl phosphate disodium substrate was then added and the reaction was stopped with 3% EDTA pH 8. Absorbance was measured with a Tecan Infinite M200 PRO plate Reader (BioTek) at 405 nm. The titers were normalized with respect to the reference serum assayed in parallel and are indicated as ELISA Units/ml (EU/ml).

### 4.9. In vivo cytotoxicity assay

Groups of six C57BL/6 mice were immunized as described above. Ten days after the immunization, all mice received intravenously (i.v.) a 1:1 mixture of syngeneic splenocytes pulsed for 1 h at 37° with 5 μM of $NP_{366-377}$ peptide (ASNENMETMESS) and loaded with 0.5 μM of CFSE or pulsed with control peptide $OVA_{257-264}$ peptide (SIINFEKL) and loaded with 10 μM of CMTMR ($5 \times 10^6$ total splenocytes). After 18 h, the spleens were collected and analyzed by flow cytometry to determine the frequencies of $CFSE^+$ and $CMTMR^+$ cells. The specific lysis was determined as previously reported [54]: 100 − ((percentage of $CFSE^+$ cells in immunized mice/percentage of $CMTMR^+$ cells in immunized mice)/

(percentage of $CFSE^+$ cells in PBS control mice/ percentage of $CMTMR^+$ cells in PBS control mice) × 100).

### 4.10. Influenza virus challenge

Groups of eight C57BL/6 mice were immunized as described above. Four weeks after the immunization, mice were anesthetized with inhalational isoflurane (4% for the induction and 1.5% for the maintenance) and then challenged intranasally with a lethal dose of Influenza A virus (strain A/Puerto Rico/8/1934 H1N1) (3000 TCID50) mouse-adapted (15 µl per nostril). Survival, body weight and clinical signs of illness (e.g. ruffled fur, hunched posture, hypothermia, body weight loss, and wheeze) were monitored daily for two weeks after the infection. A clinical score of 4 and a body weight loss superior than 20% of the initial weight were defined as humane endpoint; animals meeting these criteria were euthanized. Since NP immunization does not confer sterilizing immunity, mice with no body weight loss have been considered not properly infected and excluded from the analysis.

### 4.11. Statistical analysis

Statistical analyses were performed using GraphPad Prism 7.0 software. Experiments involving animal survival were analyzed by Mantel-Cox Log-rank test. For the other statistical analyses, Mann-Whitney *U* test was used. P values <0.05 were considered statistically significant. *, $P < 0.05$; **, $P < 0.01$.

## Acknowledgements

The authors wish to thank Simona Mangiavacchi for coordinating the delivery of formulations for the animal studies; Simona Tavarini and Chiara Sammicheli for assistance in FACS analysis; Alessandra Anemona for support in the statistical analysis; the Laboratory for Animal Services team for carrying out the animal immunizations and sample collection (all employed by GSK Vaccines at the time of the study).

## Conflict of interest

This study was sponsored by Novartis Vaccines, now acquired by the GSK group of companies, which was involved in all stages of the study conduct and analysis. MB, DP, MT, UDO, DM and EF were employees of Novartis Vaccines at the time of the study. UDO and DM report ownership of GSK shares and/or restricted GSK shares. Cristina Manara was a PhD student at the University of Rome La Sapienza. Cristina Manara PhD was sponsored by GlaxoSmithKline Biologicals SA. Following the acquisition of Novartis Vaccines by the GSK group of companies in March, 2015, CM, MB, DP, MT, UDO, DM and EF are now employees of the GSK group of companies.

## Authors' contribution

CM, MB, DP, EF contributed to the conception, design and planning of the study. CM, MB, MT and EF contributed to the collection of the data. CM, MB, DP and EF contributed to the analysis and interpretation of the results. All authors were involved in drafting the manuscript or revising it critically for important intellectual content. All authors had full access to the data and approved the manuscript before it was submitted by the corresponding author. All authors attest they meet the ICMJE criteria for authorship.

## Appendix A. Supplementary material

Supplementary data to this article can be found online at https://doi.org/10.1016/j.vaccine.2019.04.028.

## References

[1] Geall AJ, Mandl CW, Ulmer JB. RNA: the new revolution in nucleic acid vaccines. Semin Immunol 2013;25:152–9.
[2] Pascolo S. Messenger RNA-based vaccines. Expert Opin Biol Ther 2004;4:1285–94.
[3] Ulmer JB, Mason PW, Geall A, Mandl CW. RNA-based vaccines. Vaccine 2012;30:44148.
[4] Petsch B, Schnee M, Vogel AB, Lange E, Hoffmann B, Voss D, et al. Protective efficacy of *in vitro* synthesized, specific mRNA vaccines against influenza A virus infection. Nat Biotechnol 2012;30:1210–6.
[5] Geall AJ, Verma A, Otten GR, Shaw CA, Hekele A, Banerjee K, et al. Nonviral delivery of self-amplifying RNA vaccines. Proc Natl Acad Sci USA 2012;109:14604–9.
[6] Bogers WM, Oostermeijer H, Mooij P, Koopman G, Verschoor EJ, Davis D, et al. Potent immune responses in rhesus macaques induced by nonviral delivery of a self-amplifying RNA vaccine expressing HIV type 1 envelope with a cationic nanoemulsion. J Infect Dis 2015;211:947–55.
[7] Heidenreich R, Jasny E, Kowalczyk A, Lutz J, Probst J, Baumhof P, et al. A novel RNA-based adjuvant combines strong immunostimulatory capacities with a favorable safety profile. Int J Cancer J Int du Cancer 2015;137:372–84.
[8] Deering RP, Kommareddy S, Ulmer JB, Brito LA, Geall AJ. Nucleic acid vaccines: prospects for non-viral delivery of mRNA vaccines. Expert Opin Drug Deliv 2014;11(6):885–99.
[9] Ulmer JB, Geall AJ. Recent innovations in mRNA vaccines. Curr Opin Immunol 2016;41:18–22.
[10] Ulmer JB, Mansoura MK, Geall AJ. Vaccines 'on demand': science fiction or a future reality. Expert Opin Drug Discov 2015;10(2):101–6.
[11] Kallen KJ, Heidenreich R, Schnee M, Petsch B, Schlake T, Thess A, et al. A novel, disruptive vaccination technology: self-adjuvanted RNActive(®) vaccines. Hum Vaccin Immunother 2013;9(10):2263–76.
[12] Kowalczyk A, Doener F, Zanzinger K, Noth J, Baumhof P, Fotin-Mleczek M, et al. Self-adjuvanted mRNA vaccines induce local innate immune responses that lead to a potent and boostable adaptive immunity. Vaccine 2016;34(33):3882–93.
[13] Maruggi G, Chiarot E, Giovani C, Buccato S, Bonacci S, Frigimelica E, et al. Immunogenicity and protective efficacy induced by self-amplifying mRNA vaccines encoding bacterial antigens. Vaccine 2017;35(2):361–8.
[14] Cu Y, Broderick KE, Banerjee K, Hickman J, Otten G, Barnett S, et al. Enhanced delivery and potency of self-amplifying mRNA vaccines by electroporation in situ. Vaccines (Basel) 2013;1(3):367–83.
[15] Magini D, Giovani C, Mangiavacchi S, Maccari S, Cecchi R, Ulmer JB, et al. Self-amplifying mRNA vaccines expressing multiple conserved influenza antigens confer protection against homologous and heterosubtypic viral challenge. PLoS ONE 2016;11(8):e0161193.
[16] Brazzoli M, Magini D, Bonci A, Buccato S, Giovani C, Kratzer R, et al. Induction of broad-based immunity and protective efficacy by self-amplifying mRNA vaccines encoding influenza virus hemagglutinin. J Virol 2015;90(1):332–44.
[17] Hekele A, Bertholet S, Archer J, Gibson DG, Palladino G, Brito LA, et al. Rapidly produced SAM® vaccine against H7N9 influenza is immunogenic in mice. Emerg Microbes Infect 2013;2:e52.
[18] Lazzaro S, Giovani C, Mangiavacchi S, Magini D, Maione D, Baudner B, et al. CD8 T-cell priming upon mRNA vaccination is restricted to bone-marrow-derived antigen-presenting cells and may involve antigen transfer from myocytes. Immunology 2015;146(2):312–26.
[19] Liu J, Kjeken R, Mathiesen I, Barouch DH. Recruitment of antigen-presenting cells to the site of inoculation and augmentation of human immunodeficiency virus type 1 DNA vaccine immunogenicity by *in vivo* electroporation. J Virol 2008;82(11):5643–9.
[20] Barouch DH. Rational design of gene-based vaccines. J Pathol 2006;208(2):283–9.
[21] Liu Y, Xiao L, Joo KI, Hu B, Fang J, Wang P. In situ modulation of dendritic cells by injectable thermosensitive hydrogels for cancer vaccines in mice. Biomacromolecules 2014;15(10):3836–45.
[22] Sumida SM, McKay PF, Truitt DM, Kishko MG, Arthur JC, Seaman MS, et al. Recruitment and expansion of dendritic cells *in vivo* potentiate the immunogenicity of plasmid DNA vaccines. J Clin Invest 2004;114(9):1334–42.
[23] McKay PF, Barouch DH, Santra S, Sumida SM, Jackson SS, Gorgone DA, et al. Recruitment of different subsets of antigen-presenting cells selectively modulates DNA vaccine-elicited CD4+ and CD8+ T lymphocyte responses. Eur J Immunol 2004;34(4):1011–20.
[24] Taglietti M. Vaccine adjuvancy: a new potential area of development for GM-CSF. Adv Exp Med Biol 1995;378:565–9.
[25] Jones T, Stern A, Lin R. Potential role of granulocyte-macrophage colony-stimulating factor as vaccine adjuvant. Eur J Clin Microbiol Infect Dis 1994;13(Suppl 2):47–53.
[26] Warren TL, Weiner GJ. Uses of granulocyte-macrophage colony-stimulating factor in vaccine development. Curr Opin Hematol 2000;7(3):168–73.

[27] Bodey GP. The potential role of granulocyte-macrophage colony stimulating factor in therapy of fungal infections: a commentary. Eur J Clin Microbiol Infect Dis 1994;13(5):363–6.
[28] Jäger E, Ringhoffer M, Dienes HP, Arand M, Karbach J, Jäger D, et al. Granulocyte-macrophage-colony-stimulating factor enhances immune responses to melanoma-associated peptides *in vivo*. Int J Cancer 1996;67 (1):54–62.
[29] Disis ML, Bernhard H, Shiota FM, Hand SL, Gralow JR, Huseby ES, et al. Granulocyte-macrophage colony-stimulating factor: an effective adjuvant for protein and peptide-based vaccines. Blood 1996;88(1):202–10.
[30] Tarr PE, Lin R, Mueller EA, Kovarik JM, Guillaume M, Jones TC. Evaluation of tolerability and antibody response after recombinant human granulocyte-macrophage colony-stimulating factor (rhGM-CSF) and a single dose of recombinant hepatitis B vaccine. Vaccine 1996;14(13):1199–204.
[31] Kurzrock R, Talpaz M, Gutterman JU. Very low doses of GM-CSF administered alone or with erythropoietin in aplastic anemia. Am J Med 1992 Jul;93 (1):41–8.
[32] Estey EH, Kurzrock R, Talpaz M, McCredie KB, O'Brien S, Kantarjian HM, et al. Effects of low doses of recombinant human granulocyte-macrophage colony stimulating factor (GM-CSF) in patients with myelodysplastic syndromes. Br J Haematol 1991;77(3):291–5.
[33] McNeel DG, Schiffman K, Disis ML. Immunization with recombinant human granulocyte-macrophage colony-stimulating factor as a vaccine adjuvant elicits both a cellular and humoral response to recombinant human granulocyte-macrophage colony-stimulating factor. Blood 1999;93 (8):2653–9.
[34] Gerloni M, Lo D, Ballou WR, Zanetti M. Immunological memory after somatic transgene immunization is positively affected by priming with GM-CSF and does not require bone marrow-derived dendritic cells. Eur J Immunol 1998;28 (6):1832–8.
[35] Lee SW, Cho JH, Sung YC. Optimal induction of hepatitis C virus envelope-specific immunity by bicistronic plasmid DNA inoculation with the granulocyte-macrophage colony-stimulating factor gene. J Virol 1998;72 (10):8430–6.
[36] Xiang Z, Ertl HC. Manipulation of the immune response to a plasmid-encoded viral antigen by coinoculation with plasmids expressing cytokines. Immunity 1995;2(2):129–35.
[37] Kim JJ, Ayyavoo V, Bagarazzi ML, Chattergoon MA, Dang K, Wang B, et al. *In vivo* engineering of a cellular immune response by coadministration of IL-12 expression vector with a DNA immunogen. J Immunol 1997;158(2):816–26.
[38] Iwasaki A, Stiernholm BJ, Chan AK, Berinstein NL, Barber BH. Enhanced CTL responses mediated by plasmid DNA immunogens encoding costimulatory molecules and cytokines. J Immunol 1997;158(10):4591–601.
[39] Cho JH, Lee SW, Sung YC. Enhanced cellular immunity to hepatitis C virus nonstructural proteins by codelivery of granulocyte macrophage-colony stimulating factor gene in intramuscular DNA immunization. Vaccine 1999;17(9–10):1136–44.
[40] Weiss WR, Ishii KJ, Hedstrom RC, Sedegah M, Ichino M, Barnhart K, et al. A plasmid encoding murine granulocyte-macrophage colony-stimulating factor increases protection conferred by a malaria DNA vaccine. J Immunol 1998;161 (5):2325–32.
[41] Geissler M, Gesien A, Tokushige K, Wands JR. Enhancement of cellular and humoral immune responses to hepatitis C virus core protein using DNA-based vaccines augmented with cytokine-expressing plasmids. J Immunol 1997 Feb 1;158(3):1231–7.
[42] Labeur MS, Roters B, Pers B, Mehling A, Luger TA, Schwarz T, et al. Generation of tumor immunity by bone marrow-derived dendritic cells correlates with dendritic cell maturation stage. J Immunol 1999;162(1):168–75.
[43] Nestle FO, Alijagic S, Gilliet M, Sun Y, Grabbe S, Dummer R, et al. Vaccination of melanoma patients with peptide- or tumor lysate-pulsed dendritic cells. Nat Med 1998;4(3):328–32.
[44] Curiel-Lewandrowski C, Mahnke K, Labeur M, Roters B, Schmidt W, Granstein RD, et al. Transfection of immature murine bonemarrow-derived dendritic cells with the granulocyte-macrophage colony-stimulating factor gene potently enhances their *in vivo* antigen-presenting capacity. J Immunol 1999;163(1):174–83.
[45] Meropol NJ, Altmann SW, Shanafelt AB, Kastelein RA, Johnson GD, Prystowsky MB. Requirement of hydrophilic amino-terminal residues for granulocyte-macrophage colony-stimulating factor bioactivity and receptor binding. J Biol Chem 1992;267(20):14266–9.
[46] Ulmer JB, Fu TM, Deck RR, Friedman A, Guan L, DeWitt C, et al. Protective CD4+ and CD8+ T-cells against influenza virus induced by vaccination with nucleoprotein DNA. J Virol 1998;72(7):5648–53.
[47] Moskophidis D, Kioussis D. Contribution of virus-specific CD8+ cytotoxic T-cells to virus clearance or pathologic manifestations of influenza virus infection in a T-cell receptor transgenic mouse model. J Exp Med 1998;188 (2):223–32.
[48] Herrera-Rodriguez J, Meijerhof T, Niesters HG, Stjernholm G, Hovden AO, Sørensen B, et al. A novel peptide-based vaccine candidate with protective efficacy against influenza A in a mouse model. Virology 2018;515:21–8.
[49] Iavarone C, O'hagan DT, Yu D, Delahaye NF, Ulmer JB. Mechanism of action of mRNA-based vaccines. Expert Rev Vaccines 2017;16(9):871–81.
[50] Brito LA, Chan M, Shaw CA, Hekele A, Carsillo T, Schaefer M, et al. A cationic nanoemulsion for the delivery of next-generation RNA vaccines. Mol Ther 2014;22(12):2118–29.
[51] Lee SJ, Song L, Yang MC, Mao CP, Yang B, Yang A, et al. Local administration of granulocyte macrophage colony-stimulating factor induces local accumulation of dendritic cells and antigen-specific CD8+ T-cells and enhances dendritic cell cross-presentation. Vaccine 2015;33(13):1549–55.
[52] Morens DM, Fauci AS. Emerging infectious diseases: threats to human health and global stability. PLoS Pathog 2013;9(7):e1003467.
[53] Calabro S, Tortoli M, Baudner BC, Pacitto A, Cortese M, O'Hagan DT, et al. Vaccine adjuvants alum and MF59 induce rapid recruitment of neutrophils and monocytes that participate in antigen transport to draining lymph nodes. Vaccine 2011;29(9):1812–23.
[54] Stambas J, Doherty PC, Turner SJ. An *in vivo* cytotoxicity threshold for influenza A virus-specific effector and memory CD8(+) T-cells. J Immunol 2007;178 (3):1285–92.